PCCP

Accepted Manuscript

ROYAL SOCIETY OF CHEMISTRY

www.rsc.org/pccp

Formation of Dibenzofuran, Dibenozo-*p*-Dioxin and Their Hydroxylated Derivatives from Catechol

Mohammednoor Altarawneh*†, Bogdan Z. Dlugogorski

School of Engineering and Information Technology

Murdoch University, Perth, Australia

*Corresponding Author:

Phone: (+61) 8 9360-7507

E-mail: M.Altarawneh@Murdoch.edu.au

† On leave from Chemical Engineering Department, Al-Hussein Bin Talal University, Ma'an, Jordan

Abstract

We present, in this study, a mechanistic and kinetic account for the formation of dibenzofuran (DF), dibenzo-*p*-dioxin (DD) and their hydroxylated derivatives (OHs-DF/OHs-DD) from the catechol (CT) molecule, as a model compound for phenolic constituents in biomass. Self-condensation of two CT molecules produces predominantly a DD molecule via open- and closed-shell corridors. Coupling modes involving the *o*-semiquinone radical and the CT molecule (*o*-SQ/CT) generate two direct structural blocks for the formation of OHs-DF/OHs-DD structures; ether-type intermediates and di-keto moieties. Calculated reaction rate constants indicate that the fate of ether-type intermediates is to make hydroxylated diphenyl ethers rather than to undergo cyclisation reactions leading to the appearance of preDF structures. Unimolecular loss of an H or OH from pivot carbon in these hydroxylated diphenyl ethers then produces hydroxylated and non-hydroxylated DD. Formation of OHs-DF initiated by *o*(C)-*o*(C) cross-linkages involving *o*-SQ/*o*-SQ and *o*-SQ/CT reactions incur very similar reaction and activation enthalpies encountered in the emergence of chlorinated DFs from chlorophenols.

1. Introduction

Thermal processing of native and treated biomass represents a promising technique for recovery of renewable energy at industrial scale. In this field, the cutting-edge research focuses on gaining understanding of diverse chemical and physical processes occurring in pyrolysis of biomass. Great deal of this research aims at obtaining detailed mechanisms of formation and emission of oxygen-bearing pollutants. The complicated structural composition of biomass makes it difficult to link formation of organic pollutants to specific chemical reactions. To overcome the complexity germane to the structure of biomass, model compounds or surrogates are often used to mimic characteristic feature of this material.

Dihydroxylated benzenes, catechol[1] (*o*-dihydroxybenzene) and hydroquinone[2,3] (*p*-dihydroxybenzene) represent the most deployed model compounds for biomass. In particular, catechol (CT hereafter) constitues a major product from the combustion of any type of biomass, including tobacco, straw and wood. CT originates from the fission of polyphenolic constituents in lignin.[4] Degradation of CT affords the formation of anisole, phenol, benzene and hydroxylated naphthalenes.[3] Dellinger's group has thoroughly investigated thermal decomposition of CT reporting that, both pyrolytic and oxidative decomposition of CT results in the formation of dibenzo-*p*-dioxin (DD) and dibenzofuran (DF).[2,5-8] In one of the contributions of the group, Khachatryan et al.[5], using the technique of low-temperature matrix isolation electron paramagnetic resonance spectroscopy (LTMI-EPR), detected the formation of *o*-semiquinone (*o*-*SQ*) radical as the most prominent initial intermediate from decomposition of the CT molecule, via fission of one of its phenolic O-H bonds:

Scheme 1:

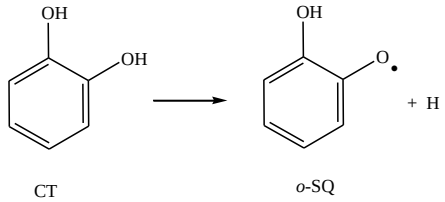

The *o-SQ* radical is often regarded as an illustrative example of the biologically damaging, reactive oxygenated species (ROS).[9] Based on available channels for the unimolecular decomposition of the *o*-SQ, we estimated its life time to be around 2200 s.[10] Due to its relatively long-life time,[10] the *o-SQ* radical has been categorised as an environmentally persistent free radical (EPFR)[3]. The term EPFR refers to radicals that have a much longer life span than most of free radicals in a combustion environment (i.e. life time of HO_2 radicals lies around 1.0 ms).[11] The long lifetime of *o*-SQ radicals enable them to serve as building blocks for the formation of DD and DF. Currently suggested mechanisms for the synthesis of DD and DF rely on the well-established analogous pathways that operate in chlorophenol systems.[3,12-16] As the opening step in these mechanisms, formation of DD and DF arises from conversion of CT into phenol. Conversely, these mechanisms do not incorporate a plausible role for the two *ortho* OH groups in mediating the occurrence of crucial reaction steps, such as ring-closure and water elimination.

The present study presents a comprehensive mechanistic account for the formation of DD and DF (and their hydroxylated derivatives) from the CT molecule and its derived *o-SQ* radical. Rate constants are determined for competing reactions to elucidate their relative importance. The results presented herein will be helpful in designing technological solutions for minimising the emissions of DD and DF from the thermal treatment of biomass.

2. Methodology

Meta hybrid density theory functional (DFT) of M062X[17] together with a moderate basis set of 6-311+G(d,p), as implemented in Gaussian09 code[18], served to perform all structural and energetic calculations. We have shown recently[19] that, energy refinement, involving single points energy calculations for a bigger basis set, changes marginally the calculated reaction and activation enthalpies (i.e. within 1.0 kcal/mol) in reference to values obtained for the 6-311+G(d,p) basis set. To test this finding for the system at hand, we found that reaction enthalpy for one selected reaction (2 catechol → 2,2'-oxydiphenol + H_2O, see Figure 1) varies by only 0.2 kcal/mol when carrying out a single point energy calculation at the extended basis set of GTLarge. To confirm further the reliability of reported thermochemistry, we calculate standard enthalpy of formation of the catechol molecule to be -66.6 kcal/mol using an isodesmic reaction (i.e. 2 phenol = catechol + benzene). Our calculated value concurs very well with estimates reported in literature[20] that vary between -63.9 kcal/mol and -66.3 kcal/mol. The nature of all transition structures was verified by calculating intrinsic reaction coordinates (IRC). The Chemrate programme[21] facilitated the computation of pressure-dependent reaction rate constants according to the RRKM/ME formalism. The buffer gas comprised N_2. The "exponential down" model utilises a $\langle \Delta E \rangle_{down}$ value at 800.0 cm^{-1}. Lennard-Jones parameters for all reactants were adapted from analogous values of phenol.[22] One-dimensional Eckart functional[23] accounted for the possible contribution from quantum tunnelling effects. One-dimensional Eckart functional[23] accounted for the possible contribution from quantum tunnelling effects. Due to the presence of hydroxyl moieties in reactants and transition structures alike, internal rotations about the O-H bonds are treated as harmonic oscillators in calculations of reaction rate constants.

3. Results and Discussions

3.1. Self-condensation of CT molecules

Figure 1 describes reaction pathways for the formation of the DD molecule initiated by self-condensation of two CT molecules. Two subsequent water elimination steps produce a DD molecule. In the initial step, the hydroxylated diphenyl ether of a 2,2'-oxydiphenol forms upon attack of the hydroxyl group of one CT molecule on the hydroxyl H atom in the other CT molecule. In the second step, a cyclisation reaction proceeds simultaneously with the extrusion of a water molecule. These two steps entail activation enthalpies of 65.2 kcal/mol (TS3) and 59.7 kcal/mol (TS8), respectively. Enthalpic barrier of TS3 resemble a corresponding barrier for HCl elimination reaction, the initial step in the bimolecular reactions of two 2-chlorophenol molecules.[24,25]

As shown in Figure 1, the OH/H radical pool could readily abstract one of the hydroxyl H atoms in the M1 molecule to yield the oxygen-centred M2 radical. An attachment of the phenoxy O in the M2 intermediate at an *ortho* site (to the C-O-C bridge), bearing either H and OH on the second phenol ring, requires very similar activation enthalpies of 17.1 kcal/mol (TS6) and 14.1 kcal/mol (TS7), respectively. Products from these two cyclisation reactions correspond to M3 and M4 adducts. Loss of H and OH from M3 and M4 intermediates affords the formation of DD and hydroxylated DD (1-OH-DD) molecules via activation enthalpies of 33.2 kcal/mol (TS10) and 35.3 kcal/mol (TS9), in that order.

Table 1 lists calculated reaction rate constants for prominent steps depicted in Figure 1 at 1.0 atm. Based on our estimated reaction rate constant, cyclisation of M2 into M4 at 800 K is ~ 5.3

times faster than the ring-closure of M2 into M3. This indicates that, formation of a DD molecule is kinetically preferred over generation of a 1-OH-DD molecule, in the open-shell pathway involving self-condensation of two CT molecules. However, the high activation enthalpy of the first step (65.2 kcal/mol) makes the self-condensation pathways of CT molecules, to produce DD and OHs-DD, not competitive with the reaction corridors described in the subsequent sections.

3.2. Products from CT/o-SQ coupling modes

In addition to the formation of the *o*-SQ radical unimolecularly through scission of one of its O-H bonds, Figure 1 shows that, H and OH radicals abstract phenoxy H atom from the CT molecule via trivial enthalpic barriers. Considering the four distinct radical sites in the *o-SQ* radical, nine distinct products (A1-A9) arise from combination of the *o-SQ* radical and its parent CT molecule, as depicted in Figure 2. Endothermicity in the range of 14.5 kcal/mol (A3) to 28.7 kcal/mol (A5) and no reaction barriers accompany the formation of the coupling products. A1, A2 and A3 species evolve from adding of the phenoxy O in the *o*-SQ radical to C(OH), *ortho* C(H) and *meta* C(H) positions in the CT molecule, respectively. *Ortho* C-C cross linkages produce the A4-A7 intermediates.

In our recent contribution,[26] we have briefly demonstrated pathways for the formation of OHs-DF structures from A1 and A2 adducts. Herein, we account for the formation of OHs-DD/OHs-DF from A3 and A4-A7 intermediates. Due to the presence of the phenoxy functional group in *ortho* positions with respect to the C-C linkage in A8 and A9 intermediates, these structures could not act as precursors for formation of DF(OH)s. Figure 3 shows reaction pathways

leading to the formation of DF, DD and their hydroxylated derivatives from the A1-A3 intermediates with embedded reaction and activation enthalpies pertinent to individual steps. Three exit corridors are available for A1-A3 adducts: (i) Self-ejection of H, OH and H from A2, A1 and A3 intermediates. This process affords the hydroxylated diphenyl ethers M7, M1 and M19, via sizable enthalpic barriers of 26.7 kcal/mol (TS16), 28.5 kcal/mol (TS23) and 40.5 kcal/mol (TS26), respectively. (ii) Ring-closure reactions of A2 and A1 with simultaneous elimination of water molecules. Formation of the two preDD intermediates M3 and M8 via this process requires substantial activation enthalpies of 58.0 kcal/mol (TS17) 60.1 kcal/mol (TS22), respectively. Subsequent departure of the out-of-plane H and OH in M3 and M8 leads to hydroxylated DD (1-OH-DD and DD) molecules, correspondingly. (iii) C-C cross-linkages leading to formation of preDF intermediates. In each phenyl ring in A1-A3, there exist two *ortho* potent cross-linkage sites. It follows that, there are four plausible C-C bridging-type reaction products for A2 (preDF1-preDF4), four for A1 (preDF5-preDF8) and two for A3 (preDF9-preDF10). Formation of these ten preDF intermediates is slightly endothermic (10.5 kcal/mol – 20.7 kcal/mol) and requires activation enthalpies in the narrow range of 26.5-38.6 kcal/mol (TS12-TS15, TS18-TS21 and TS24-TS25). As shown in Figure 3, DF and its hydroxylated derivatives arise from preDF intermediates via water elimination reactions (TS28-TS31, TS33), hydrogen elimination (TS27) and unimolecular loss of out-of-plane H or OH moieties.

Based on calculated enthalpic barriers of the three available exit channels for A1-A3 structures, it is apparent that the fate of A1-A3 is most likely to be controlled by either C-C cross-linkage reaction or direct fission of C-H/OH from their ether bridges. The exceedingly high barriers associated with unimolecular elimination of H_2O shut down this channel. In order to elucidate the relative importance of C-C cross-linkages leading to the formation of preDF intermediates

in comparison with H/OH self-ejection resulting in the production of hydroxylated diphenyl ethers, in Table 1, we report the fitted reaction rate constants for these two groups of reactions. Figure 4 presents branching ratios for the exit channels of A1, A2 and A3 intermediates at 1.0 atm. In calculations of these reaction rate constants, we treat potential rotations about C-O bonds in A1, A2 and A3 radicals as hindered rotors (HR). Figure S1 in the supporting information portrays their associated rotor potentials. We find that, the HR treatment affords reaction rate constants that are lower by factors of 2.51, 2.13 and 1.15, pertinent to the formation of the preDF intermediates from A1, A2 and A3, respectively, if compared with the harmonic oscillator approach. This is expected in view of the significant loss of entropy accompanying the formation of the "rotationally-locked" transition states (i.e. TS12-TS15, TS18-TS21 and TS24-TS25).

It is apparent that fission of C-H and OH in A1 and A2 intermediates bonds holds significantly more importance than C-C bridging reactions at all temperature. The overall contributions of channels leading to the formation of preDF intermediates from A1 and A2 structures at 800 K amount to ~ 27.0 % and ~ 7.0 % where major preDF structures comprise preDF2 and preDF6, correspondingly. It follows that, addition of the phenoxy O atom in a *o*-SQ radical to ortho C(H) or C(OH) sites in a CT molecule leads principally to the formation of hydroxylated diphenyl ethers (M1 and M7). As shown in the previous section, an open-shell pathway operates via a facile mechanism to convert hydroxylated diphenyl ethers (e.g., M1, A2) into DD and 1-OH-DD molecules. In case of the A3 structure, formation of the preDF10 intermediate is predicted to be more significant than that of a C-H bond fission (i.e. formation of the M19 molecule) up to ~ 700 K.

Formation of DF and its hydroxylated derivatives from the keto-keto intermediates of A4-A7 follows analogous mechanisms to those operating in the production of polychlorinated DFs from chlorinated phenoxy radicals; *o*(C)-*o*(C) cross-linkages, single or double enolisation and cyclisation accompanied with water elimination. Figure 5 maps out reaction steps involved in the formation of 4,6-DiOH-DF molecule starting from the A4 intermediate. The uppermost pathway depicts a closed-shell mechanism while the lowermost pathway in Figure 5 shows an open-shell mechanism. The open-shell pathway is most likely to be hindered in view of the tremendous enthalpic barriers of the enolisation step (63.0 kcal/mol) and ring-closure occurring simultaneously with water elimination (79.5 kcal/mol). In the closed-shell pathway, ring-closure and water elimination steps require activation enthalpies of 45.2 kcal/mol (TS34) and 52.5 kcal/mol (TS35), respectively.

3.3. Products from self-condensations of o-SQ /o-SQ

Figure 6 displays nine products from self-condensation of two *o*-SQ radicals. These products feature attachment of phenoxy O in one *o*-SQ radical to the two *ortho* positions in the other o-SQ (A13 and A14), and the three plausible *ortho* C-C coupling products (A10-A12). Couplings involving *para* sites as in A15-A18 structures are not relevant to the formation of DF/DF. Formation of the dihydroxylated diketo A12 is thermodynamically more preferred than formation of the other two keto-keto adducts (A10 and A11). Likewise, attachment of the phenoxy O at an *o*-C(H) site acquires slightly more exothermicity than the corresponding attachment at an *o*-C(OH) site. Clearly, A10-A12 intermediates serve as building blocks for production of OHs-DF, while A13-A14 structures are precursors for the formation of OHs-DD. Formation of hydroxylated DFs from A10-A12 intermediate follows the well-known

equivalent mechanism in chlorophenol systems. Figure 7 depicts pathways for the formation of 4,6-DiOH-DF, 4-OH-DF, 1-OH-DD and 1,9-DiDD molecules initiated by unimolecular arrangements of the intermediates A12, A11, and A14 respectively. It is deduced from pathways in Figures 5 and 7 that, energetics of the formation of OHs-DF in the CT system concur with corresponding values encountered in the formation of chlorinated DFs from chlorophenols. Loss of a hydroxyl moiety from the A13 structure forms the intermediate M2, which could undergo ring-closure reactions to produce DD and 1-OH-DD molecules as shown in Figure 1. These pathways also operate in the transformation of the M24 adduct into 1-OH-DD and 1,9-DiDD molecules (Figure 7c).

3.4. Comparison with other mechanisms

Central to all mechanisms operating in the formation of DD from substituted phenols is the open shell ring-closure reaction:

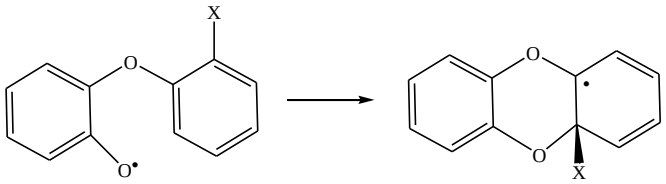

We find that activation enthalpy for this reaction is sensitive to the atomic substituent at the *ortho* position (X). We calculate activation enthalpies to be 27.3 kcal/mol, 27.0 kcal/mol, 24.7 kcal/mol and 22.0 kcal/mol for X = Cl, Br, H and OH, respectively. Figure 8 provides Arrhenius plots for these four cyclisation reactions at 1.0 atm. Ring-closure toward an *ortho* C(OH) site (i.e. relevant to the CT system) is predicted to be faster than ring-closures toward C(Cl), C(Br) and C(H) sites by 55.0, 12.5 and 4.5 times, respectively. Consequently, we

envisage that oxidation/pyrolysis of CT to form DD molecules at a faster rate than corresponding systems of chlorophenols, bromophenols and phenols.

Along the same line of enquiry, bottleneck step in formation of halogenated DF congeners from substituted phenols is the first enolisation step from a keto-keto mesomer into an enol-keto intermediate:

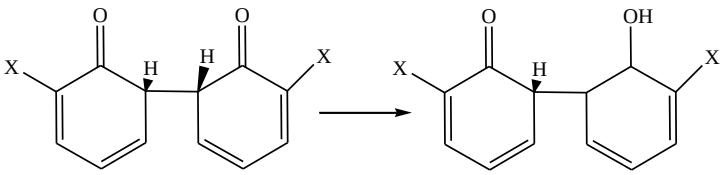

Reported barrier of this step varies from 60.0 kcal/mol to 70.0 kcal/mol.[13,14,16,25] We find that the presence of two OH substituents at *ortho* positions does not influence this high barrier (i.e barrier height of TS38) in reference to the values reported in literature for H, Cl and Br *ortho* substituents. We have made several unsuccessful attempts to find a lower activation barrier for this step via simultaneous migrations of H atoms taking advantage of the presence of *ortho* OH substituents (as in A11 and A12). Nevertheless, we have shown in Section 3.2 that, C-C cross-linkages of initial CT/*o*-SQ intermediates incur significantly lower activation enthalpies (i.e. 26.0 kcal/mol – 34.0 kcal/mol) and lead to the formation of preDF structures. To the best of our knowledge, our discussed C-C ring-closure reactions have never been proposed as pathways for the formation of substituted DF molecules.

Overall, our theoretical modelling predicts formation of hydroxylated derivatives of DF and DF in parallel competing routes to those of DF and DD. However, Dellinger's group did not detect their formation under various operational conditions. A plausible elucidation for their absence, besides complications with the gas-chromatography analysis, is their expected prompt decomposition in an analogy to the well-established mechanism of the thermal decomposition

of phenol, i.e., ring contraction/CO elimination mechanism.[27] Furthermore, pyrolysis of biomass proceeds in a highly reducing environment. We have previously shown that the replacement of OH groups by H atoms in the CT molecule is associated with an energy barrier very similar to that of phenolic H abstraction.[28] Clearly, both processes have the potential to consume OHs-DF/OHs-DD.

4. Conclusions

This contribution presented mechanistic pathways underpinning the formation of DF/DD and their hydroxylated derivatives from bimolecular reactions involving CT with *o-SQ* radical as model compounds for structural entities in biomass. Bimolecular reactions involving CT molecules are found to afford solely DD and 1-OH-DD, requiring high activation energy for the initial condensation step. Low energy pathways are illustrated for the formation of DF, DD, OHs-DF and OHs-DD from CT/o-SQ and o-SQ/o-SQ coupling reactions. Unimolecular loss of an H or OH from pivot carbon linkage in ether-type adducts is predicted to be kinetically preferred over the condensation pathways for the formation of DD and OHs-DD, whereas DF and OHs-DF appear as a consequence of creation of *o*(C)-*o*(C) linkages in the CT/o-SQ coupling modes.

Supporting Information Available

Figure S1, Cartesian coordinates for transition structures.

Conflict of Interest: The authors declare that they have no conflict of interest.

Acknowledgement

This study has been supported by a grant of computing time from the National Computational Infrastructure (NCI), Australia as well as funds from the Australian Research Council (ARC).

References

(1) Lomnicki, S.; Truong, H.; Dellinger, B. Mechanisms of Product Formation from the Pyrolytic Thermal Degradation of Catechol, *Chemosphere* **2008**, *73*, 629.
(2) Khachatryan, L.; Asatryan, R.; McFerrin, C.; Adounkpe, J.; Dellinger, B. Radicals from the Gas-Phase Pyrolysis of Catechol. 2. Comparison of the Pyrolysis of Catechol and Hydroquinone, *J. Phys. Chem. A* **2010**, *114*, 10110.
(3) Truong, H.; Lomnicki, S.; Dellinger, B. Mechanisms of Molecular Product and Persistent Radical Formation from the Pyrolysis of Hydroquinone, *Chemosphere* **2008**, *71*, 107.
(4) Kibet, J.; Khachatryan, L.; Dellinger, B. Molecular Products and Radicals from Pyrolysis of Lignin, *Environ. Sci. Technol.* **2012**, *46*, 12994.
(5) Khachatryan, L.; Adounkpe, J.; Asatryan, R.; Dellinger, B. Radicals from the Gas-Phase Pyrolysis of Catechol: 1. O-Semiquinone and Ipso-Catechol Radicals, *J. Phys. Chem. A* **2010**, *114*, 2306.
(6) Khachatryan, L.; Adounkpe, J.; Maskos, Z.; Dellinger, B. Formation of Cyclopentadienyl Radical from the Gas-Phase Pyrolysis of Hydroquinone, Catechol, and Phenol, *Environ. Sci. Technol.* **2006**, *40*, 5071.
(7) Khachatryan, L.; Dellinger, B. Environmentally Persistent Free Radicals (Epfrs)-2. Are Free Hydroxyl Radicals Generated in Aqueous Solutions?, *Environ. Sci. Technol.* **2011**, *45*, 9232.
(8) Khachatryan, L.; Vejerano, E.; Lomnicki, S.; Dellinger, B. Environmentally Persistent Free Radicals (EPFRs). 1. Generation of Reactive Oxygen Species in Aqueous Solutions, *Environ. Sci. Technol.* **2011**, *45*, 8559.
(9) Dellinger, B.; Khachatryan, L.; Masko, S.; Lomnicki, S. Free Radicals in Tobacco Smoke, *Mini-Rev. Org. Chem.* **2011**, *8*, 427.

(10) Altarawneh, M.; Dlugogorski, B. Z.; Kennedy, E. M.; Mackie, J. C. Thermochemical Properties and Decomposition Pathways of Three Isomeric Semiquinone Radicals, *J. Phys. Chem. A* **2009**, *114*, 1098.

(11) Dellinger, B.; Khachatryan, L.; Masko, S.; Lomnicki, S. Free Radicals in Tobacco Smoke, *Mini. Rev. Org. Chem.* **2011**, *8*, 427.

(12) Altarawneh, M.; Dlugogorski, B. Z. A Mechanistic and Kinetic Study on the Formation of PBDD/Fs from PBDEs, *Environ. Sci. Technol.* **2013**, *47*, 5118.

(13) Xu, F.; Wang, H.; Zhang, Q.; Zhang, R.; Qu, X.; Wang, W. Kinetic Properties for the Complete Series Reactions of Chlorophenols with Oh Radicals—Relevance for Dioxin Formation, *Environ. Sci. Technol.* **2010**, *44*, 1399.

(14) Xu, F.; Yu, W.; Zhou, Q.; Gao, R.; Sun, X.; Zhang, Q.; Wang, W. Mechanism and Direct Kinetic Study of the Polychlorinated Dibenzo-P-Dioxin and Dibenzofuran Formations from the Radical/Radical Cross-Condensation of 2,4-Dichlorophenoxy with 2-Chlorophenoxy and 2,4,6-Trichlorophenoxy, *Environ. Sci. Technol.* **2010**, *45*, 643.

(15) Yu, W.; Hu, J.; Xu, F.; Sun, X.; Gao, R.; Zhang, Q.; Wang, W. Mechanism and Direct Kinetics Study on the Homogeneous Gas-Phase Formation of PPDD/Fs from 2-BP, 2,4-DBP, and 2,4,6-Tbp as Precursors, *Environ. Sci. Technol.* **2011**, *45*, 1917.

(16) Zhang, Q.; Yu, W.; Zhang, R.; Zhou, Q.; Gao, R.; Wang, W. Quantum Chemical and Kinetic Study on Dioxin Formation from the 2,4,6-Tcp and 2,4-DCP Precursors, *Environ. Sci. Technol.* **2010**, *44*, 3395.

(17) Zhao, Y.; Truhlar, D. The M06 Suite of Density Functionals for Main Group Thermochemistry, Thermochemical Kinetics, Noncovalent Interactions, Excited States, and Transition Elements: Two New Functionals and Systematic Testing of Four M06-Class Functionals and 12 Other Functionals, *Theor Chem Account* **2008**, *120*, 215.

(18) Frisch, M. J. T., G. W.; Schlegel, H. B.; Scuseria, G. E.; Robb, M. A.; Cheeseman, J. R.; Scalmani, G.; Barone, V.; Mennucci, B.; Petersson, G. A.; Nakatsuji, H.; Caricato, M.; Li, X.; Hratchian, H. P.; Izmaylov, A. F.; Bloino, J.; Zheng, G.; Sonnenberg, J. L.; Hada, M.; Ehara, M.; Toyota, K.; Fukuda, R.; Hasegawa, J.; Ishida, M.; Nakajima, T.; Honda, Y.; Kitao, O.; Nakai, H.; Vreven, T.; Montgomery, Jr., J. A.; Peralta, J. E.; Ogliaro, F.; Bearpark, M.; Heyd, J. J.; Brothers, E.; Kudin, K. N.; Staroverov, V. N.; Kobayashi, R.; Normand, J.; Raghavachari, K.; Rendell, A.; Burant, J. C.; Iyengar, S. S.; Tomasi, J.; Cossi, M.; Rega, N.; Millam, J. M.; Klene, M.; Knox, J. E.; Cross, J. B.; Bakken, V.; Adamo, C.; Jaramillo, J.; Gomperts, R.; Stratmann, R. E.; Yazyev, O.; Austin, A. J.; Cammi, R.; Pomelli, C.; Ochterski, J. W.; Martin, R. L.; Morokuma, K.; Zakrzewski, V. G.; Voth, G. A.; Salvador, P.; Dannenberg, J. J.; Dapprich, S.; Daniels, A. D.; Farkas, Ö.; Foresman, J. B.; Ortiz, J. V.; Cioslowski, J.; Fox, D. J. ; A.1 ed.; Gaussian, Inc: Wallingford CT, 2009.

(19) Altarawneh, M.; Dlugogorski, B. Z. Mechanism of Thermal Decomposition of Tetrabromobisphenol a (TBBA), *J. Phys. Chem. A* **2014**, *118*, 9338.

(20) Gonçalves, E. M.; Agapito, F.; Almeida, T. S.; Martinho Simões, J. A. Enthalpies of Formation of Dihydroxybenzenes Revisited: Combining Experimental and High-Level Ab Initio Data, *J. Chem. Thermodyn.* **2014**, *73*, 90.

(21) Mokrushin, V. B., V.; Tsang, W.; Zachariah, M.; Knyazev, V; ChemRate. V.1.19 ed.; NIST: Gaithersburg, MD, 2002.

(22) *Rc Handbook of Chemistry and Physics: A Ready-Reference Book of Chemical and Physical Data*; CRC, Boca Raton: London, 2008.

(23) Eckart, C. The Penetration of a Potential Barrier by Electrons, *Phys. Rev.* **1930**, *35*, 1303.

(24) Altarawneh, M.; Dlugogorski, B. Z.; Kennedy, E. M.; Mackie, J. C. Quantum Chemical Investigation of Formation of Polychlorodibenzo-P-Dioxins and Dibenzofurans from Oxidation and Pyrolysis of 2-Chlorophenol, *J. Phys. Chem. A* **2007**, *111*, 2563.

(25) Altarawneh, M.; Dlugogorski, B. Z.; Kennedy, E. M.; Mackie, J. C. Mechanisms for Formation, Chlorination, Dechlorination and Destruction of Polychlorinated Dibenzo-P-Dioxins and Dibenzofurans (Pcdd/Fs), *Prog. Energy Combus. Sci.* **2009**, *35*, 245.

(26) Altarawneh, M.; Dlugogorski, B. Z. Formation of Dibenzo-*P*-Dioxin and Dibenzofuran from Catechol in Relevance to Combustion of Biomass, *Organohalogen Compd.* **2014**, *In press.*

(27) Altarawneh, M.; Dlugogorski, B. Z.; Kennedy, E. M.; Mackie, J. C. Quantum Chemical Study of Low Temperature Oxidation Mechanism of Dibenzofuran, *J. Phys. Chem. A* **2006**, *110*, 13560.

(28) Altarawneh, M.; Dlugogorski, B. Z.; Kennedy, E. M.; Mackie, J. C. Theoretical Study of Unimolecular Decomposition of Catechol, *J. Phys. Chem. A* **2009**, *114*, 1060.

Table 1: Fitted modified Arrhenius reaction rate parameters ($k(T) = AT^n\exp(-E_a/RT)$) (between 400 – 1600 K) at 1.0 atm for selected unimolecular exit channels of A1, A2 and A3 intermediates.

Reaction	A (s^{-1}, molecule, cm^3)	E_a (cal/mol)
M2 → M3	4.79×10^{10}	23 200
M2 → M4	6.31×10^{10}	20 900
A1 → preDF1	2.35×10^{9}	25 300
A1 → preDF2	7.77×10^{10}	24 400
A1 → preDF3	3.90×10^{9}	26 000
A1 → preDF4	2.69×10^{9}	23 900
A1 → M7 + H	1.91×10^{11}	23 900
A2 → preDF5	8.50×10^{19}	28 800
A2 → preDF6	3.03×10^{10}	24 600
A2 → preDF7	1.15×10^{9}	24 100
A2 → preDF8	3.40×10^{9}	23 100
A2 → M1 + OH	5.80×10^{11}	25 000
A3 → preDF9	2.28×10^{11}	37 600
A3 → preDF10	1.00×10^{11}	33 700
A3 → M19 + H	1.10×10^{13}	40 400

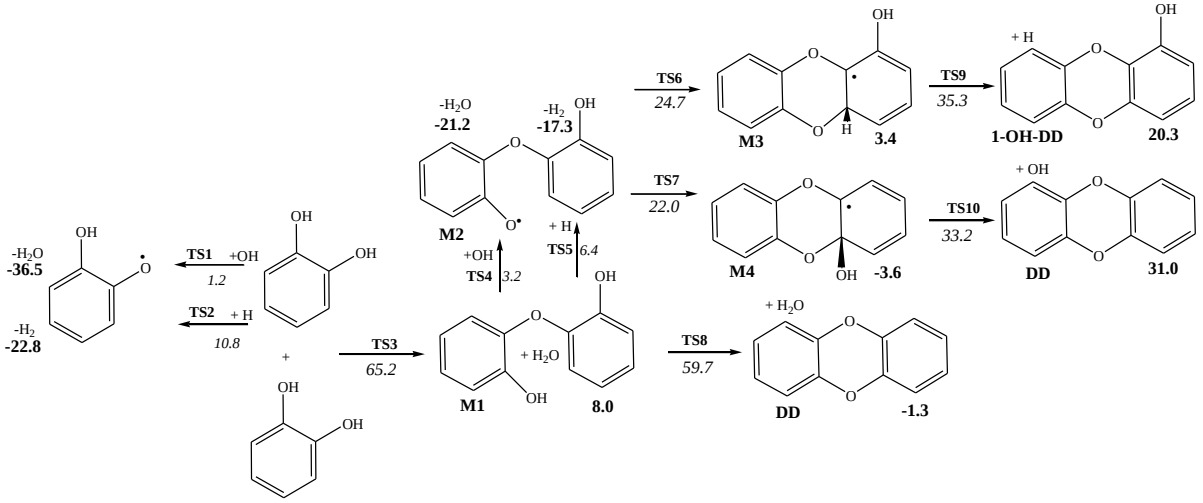

423

424 **Figure 1:** Pathways to formation of DD and 1-OH-DD molecules from self-condensation of

425 two CT molecules. Values in bold and italic denote reaction and activation enthalpies,

426 respectively.[17] All values are in kcal/mol, as calculated at 298.15 K.

427

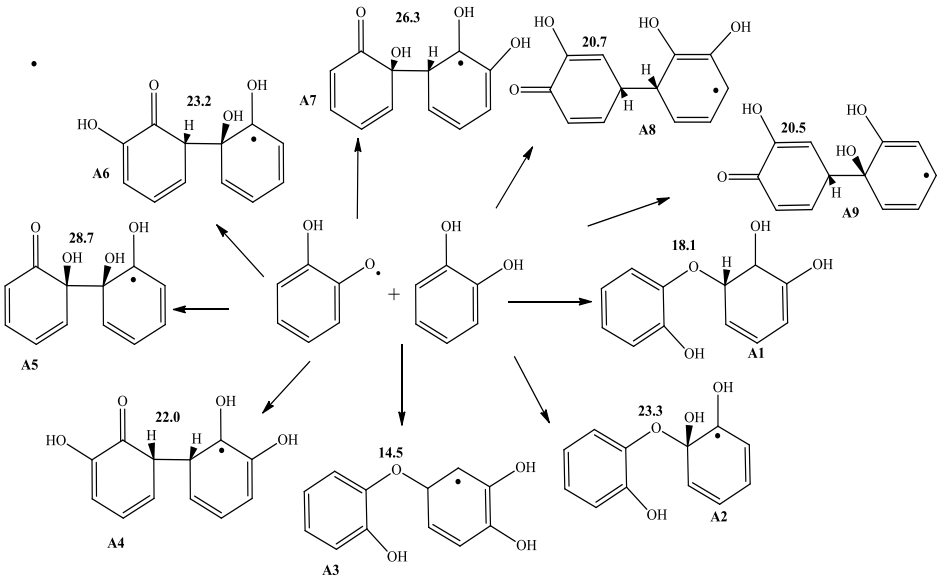

Figure 2: Initial products from *o*-SQ/CT coupling modes. Values in bold signify reaction enthalpies at 298.15 K (in kcal/mol).

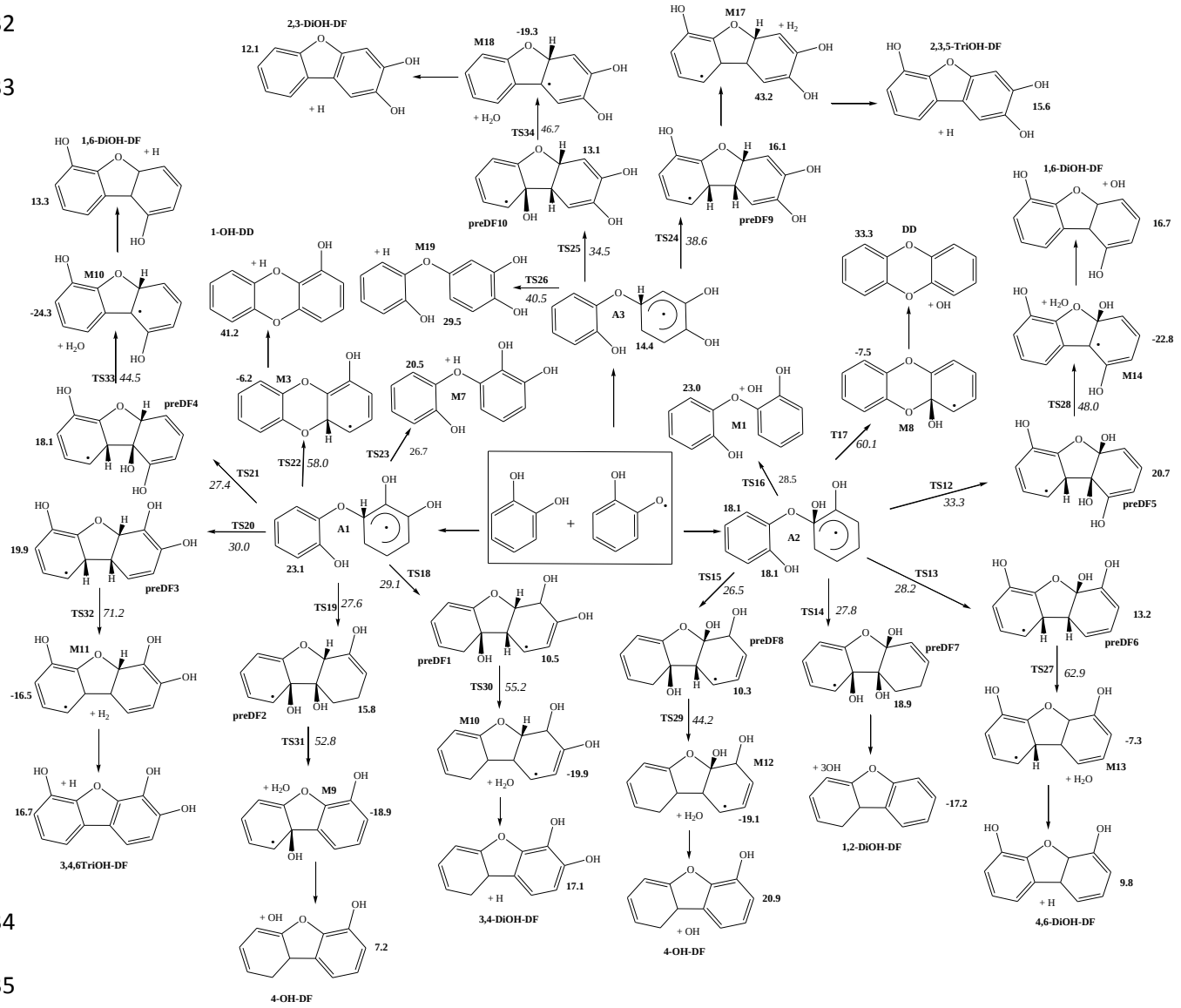

Figure 3: Pathways to products from three o-SQ/CT coupling species. Values in bold and italic denote reaction and activation enthalpies, respectively. All values are in kcal/mol calculated as at 298.15 K. Pathways involving A1 and A2 are from reference 17.

(a)

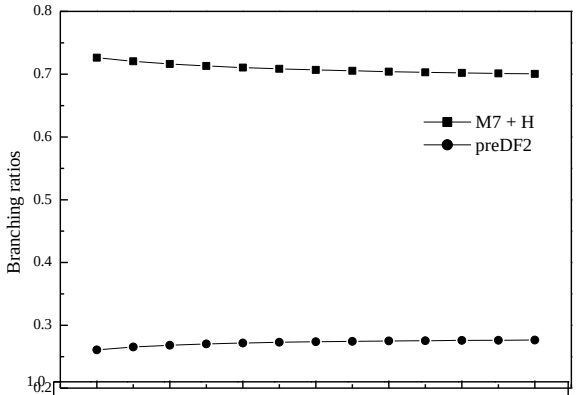

(b)

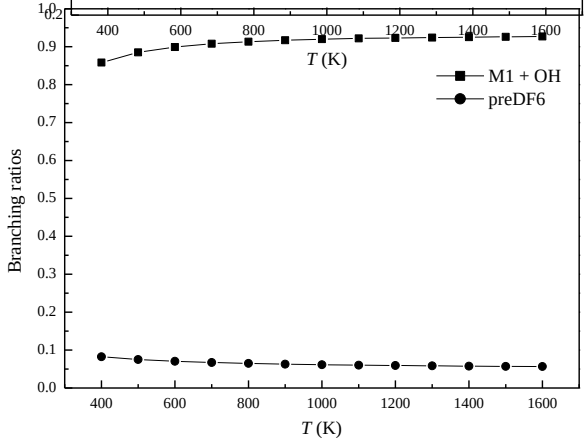

(c)

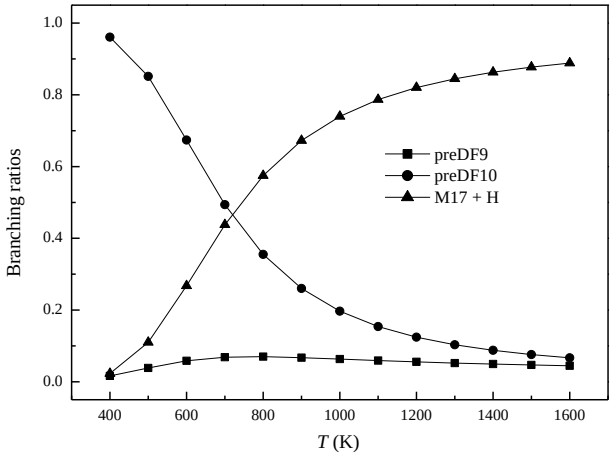

Figure 4: Branching ratios at 1.0 atm for formation of preDF structures and hydroxylated diphenyl ethers from o-SQ/CT coupling products of A1 (a), A2 (b) and A3 (c). Branching ratios for the channels, which are not shown for A1 and A2, amount to less than 2.5 %. Figure S2 in the supporting information depicts branching ratios for these minor channels.

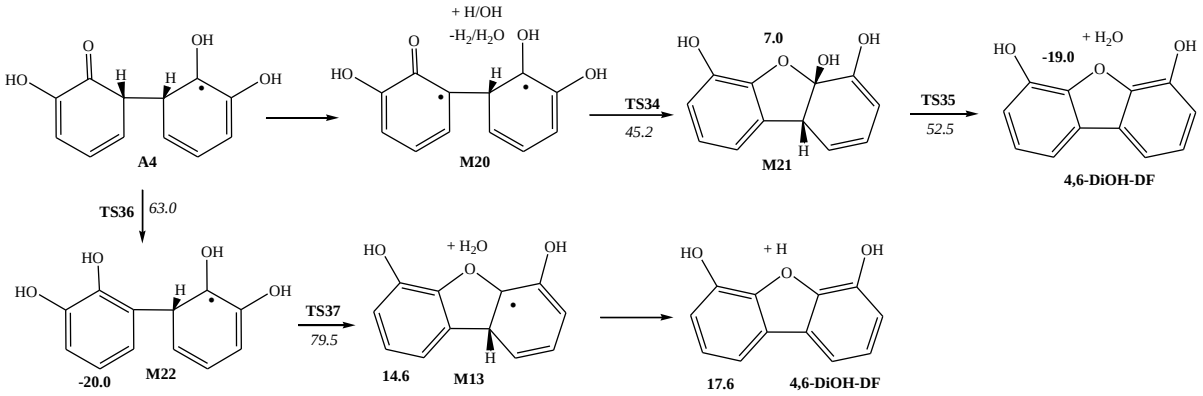

Figure 5: Formation of 4,6-DiOH-DF molecule from the *o*-SQ/CT coupling product of A4. Values in bold and italic denote reaction and activation enthalpies, respectively. All values are in kcal/mol calculated at 298.15 K.

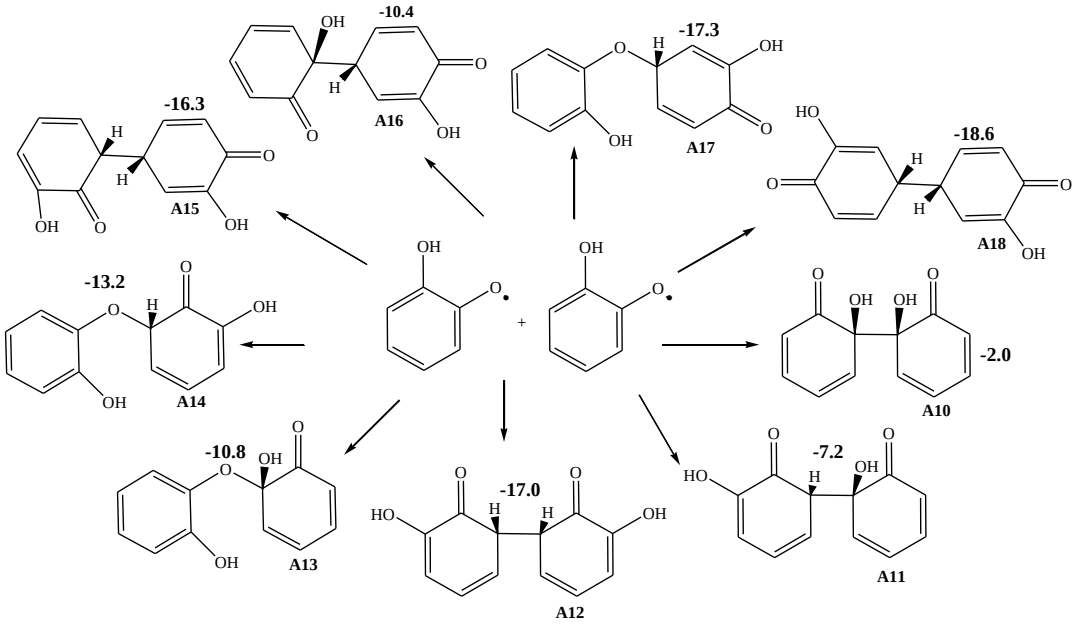

Figure 6: Products from self-condensation of *o*-SQ radicals. Values in bold signify reaction enthalpies at 298.15 K (in kcal/mol).

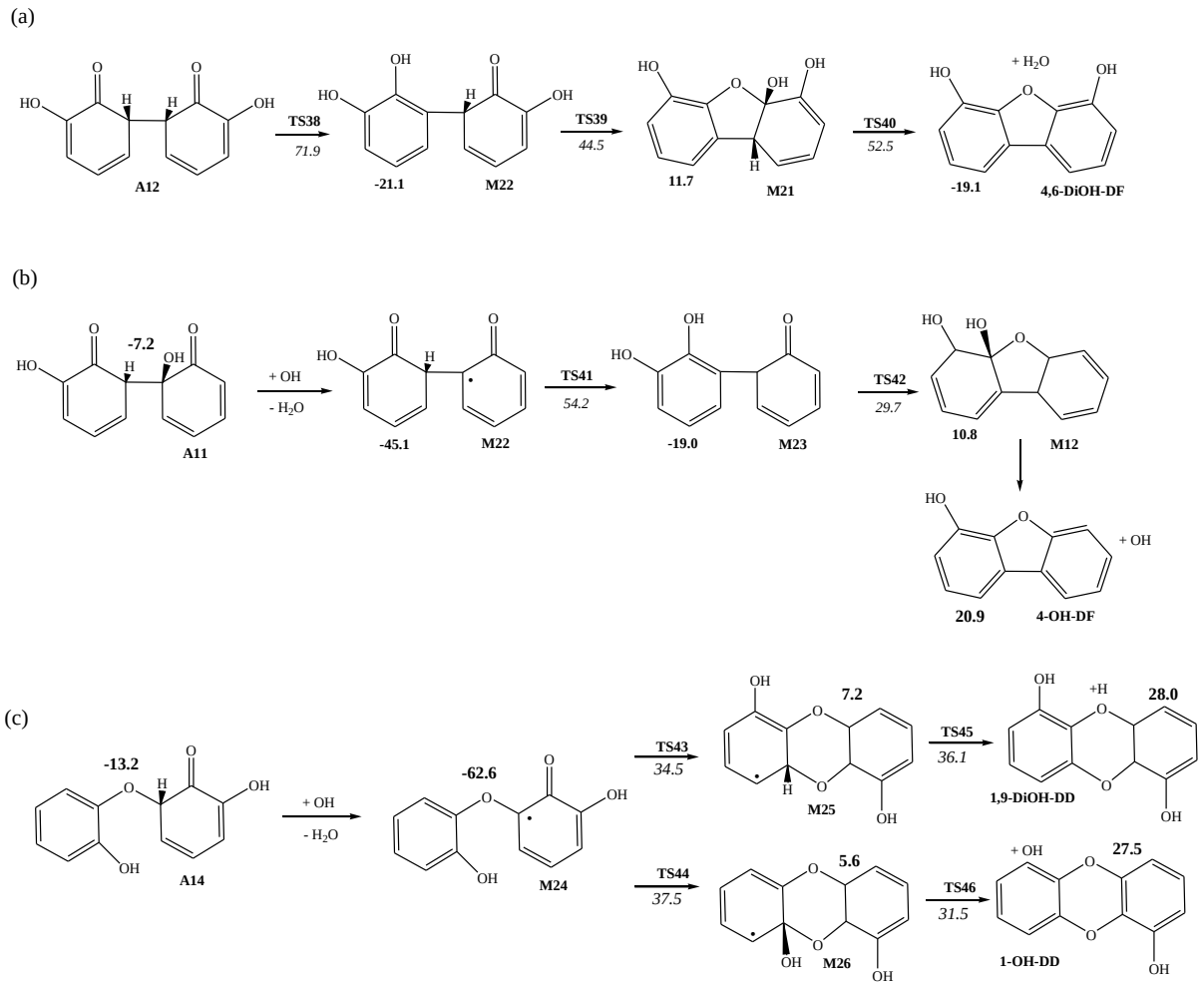

Figure 7: Pathways for the formation of 4,6-DiOH-DF (a) 4-OH-DF (b) and 1-OH-DD/1,9-DiOH-DD molecules from A12, A11 and A14 intermediates. Values in bold and italic denote reaction and activation enthalpies, respectively. All values are in kcal/mol calculated at 298.15 K.

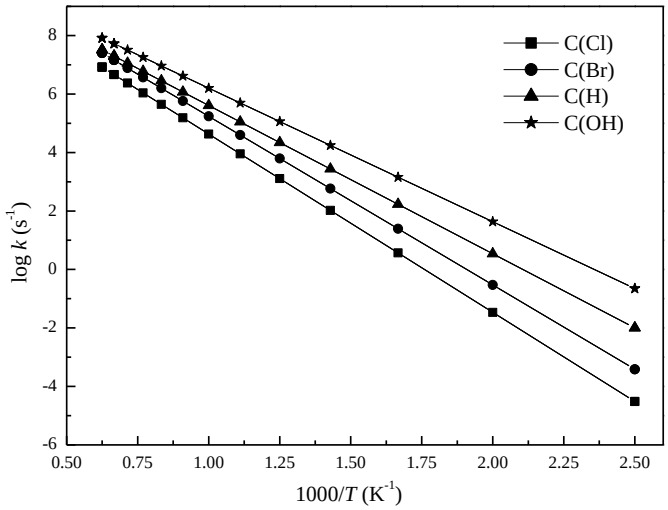

493

494 **Figure 8:** Arrhenius plots at 1.0 atm for the open-shell ring closure reactions involving *ortho*

495 substituted Cl, Br, H and OH diphenyl ether.